Brain Inspired Cognitive Systems
August 29 – September 1, 2004
University of Stirling, Scotland, UK

UNILATERAL COUPLING BETWEEN TWO MFHN ELECTRONIC NEURONS

S. Jacquir, S. Binczak* and J.M. Bilbault
LE2I, CNRS UMR 5158
Aile Sciences de l'Ingénieur
Université de Bourgogne, BP 47870
Dijon Cedex, France
*Email : stbinc@u-bourgogne.fr

V.B. Kazantsev and V.I. Nekorkin
Institute of Applied Physics of RAS
46 Uljanov str.
603950 Nizhny Novgorod, Russia

ABSTRACT

A nonlinear electrical circuit is proposed as a basic cell for modeling FitzHugh-Nagumo neurons with a modified excitability. Depending on initial conditions and parameters experiments show various dynamics including stability with excitation, bistability and oscillations. Moreover, we present an electrical circuit which will be used to realize a unidirectional coupling between two cells, mimicking chemical synaptic coupling. Finally, we characterize the frequency-doubling and the chaotic dynamics depending on the coupling strength in a master-slave configuration. In all experiments, we stress the influence of the coupling strength on the control of the slave neuron.

INTRODUCTION

Research on neural communication is based on a strong synergy between neuroscience discipline and engineering science [1, 2]. As a consequence, electrical circuits are developed including features observed in real neural systems in order to have a flexible, very fast processing and experimental medium mimicking neural activity. Famous illustrations and starting-points of electrical realizations are the Nagumo's lattice [3] and Neuristor device [1], modeling he FitzHugh-Nagumo (FHN) equation . In this case, oscillations rise from Andronov-Hopf bifurcations: Pulses can propagate with well-defined non zero minimum frequency, as observed for most axons. However, numerous nervous fibers, such as pyramidal cells in cortex or barnacle muscle fibers, are governed by a different mechanism leading to saddle homoclinic loop bifurcations [4] so that the minimum frequency of traveling waves can be close to zero [2,5].

In this paper, in the first part, we propose a nonlinear electrical circuit based on the FitzHugh-Nagumo equation with a modified excitability leading to complex dynamics of traveling waves [6, 7] emerging from saddle homoclinic loop bifurcations. Then, experimental conditions for stability with excitation threshold, bistability and oscillations are discussed.

In the second part, we use this circuit as a basic cell to realize a master-slave configuration. Two cells are coupled in a unidirectional manner, which would correspond to two neurons coupled synaptically. We present the electronic circuit giving this coupling. Then, we discuss the experimental conditions for which the master dynamics controls the excitability of the slave neuron leading to a shift of bifurcation curves, a variation of an eigen interspike frequency or a chaotic behaviour.

EXPERIMENTAL DESCRIPTION OF ONE CELL

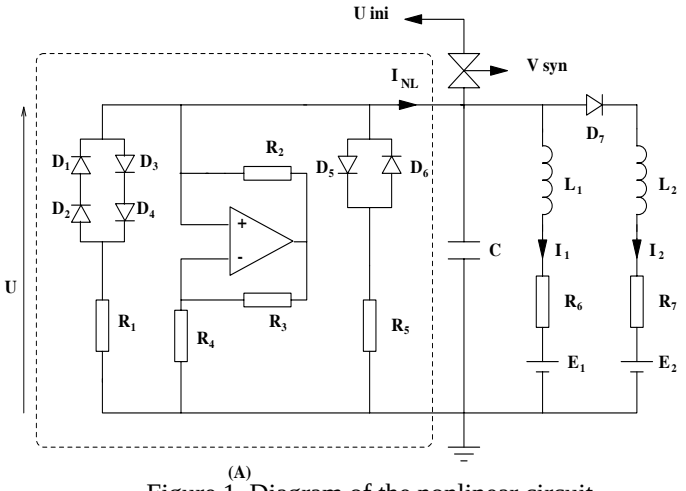

Figure 1. Diagram of the nonlinear circuit

The nonlinear circuit, as sketched in Figure 1, can be described as follows: Part (A) is a parallel association of three

different branches, two of them being resistive and commuted by silicium diodes (Vd = 0.6 V) while the third one is a negative resistor obtained with an operational amplifier.

Due to diodes' commuting behavior, the resulting I-V characteristic is nonlinear and can be modeled by a cubic polynomial function for an appropriate set of parameters so that

$$I_{NL} = f(U) = \frac{1}{R_0}\left[U - \frac{\gamma^2 U^3}{3}\right] \qquad (1)$$

where U and I_{NL} are respectively the voltage and the corresponding current. The parameters R_0 and γ are obtained by a fitting approximation, e.g. by least mean square's method. As illustrated in Figure 2, we obtain a good match between experimental results and equation (1) by setting $R_0 = 1010\,\Omega$ and $\gamma = 1.138\,V^{-1}$.

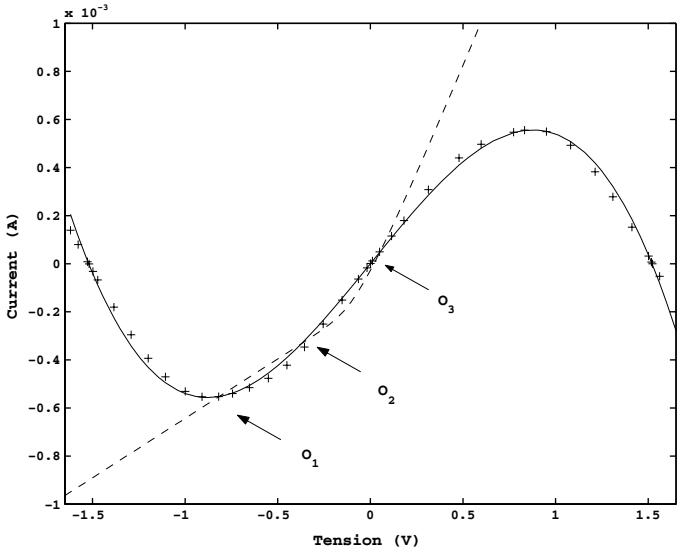

Figure 2. Experimental I-V characteristic (+ symbols) of part A. Continuous line: $I_{NL} = f(U)$ from equation (1) with $R_0 = 1010\ \Omega$ and $\gamma = 1.138 V^{-1}$. Dashed line: Experimental characteristic $(I_1 + I_2)$ versus U with $R_6 = 2021\ \Omega$, $R_7 = 690\ \Omega$, $L_1 = 10.2\ mH$, $L_2 = 3.5\ mH$ and $E_1 = 0.4\,V$.

This nonlinear resistor is connected with a capacitance and with two branches in parallel including inductances, resistances and voltage sources, one of them being commuted by a silicium diode so that setting the conditions $\frac{R_6}{L_1} = \frac{R_7}{L_2}$ and $E_2 = -V_d$, then, using a piecewise linear I-V description for diode D_7, $I_2 = 0$ if $U < 0$.

Therefore, using Kirchhoff's laws, the system of equations can be expressed in a normalized way by:

$$\begin{cases} \dfrac{dV}{d\tau} = \left[V - \dfrac{V^3}{3}\right] - W \\ \dfrac{dW}{d\tau} = \varepsilon\left[g(V) - W - \eta\right] \end{cases} \qquad (2)$$

where $V = \gamma U$ and $W = \gamma R_0 (I_1 + I_2)$ correspond, in biological terms, to the membrane voltage and the recovery variable; $\tau = \frac{t}{R_0 C}$ is a rescaled time, $\varepsilon = \frac{R_0 R_6 C}{L_1}$ the recovery parameter and $\eta = \gamma \frac{R_0}{R_6} E_1$ a bifurcation parameter. $g(V)$ is a piecewise linear function, so that $g(V) = \alpha V$ if $V \le 0$ and $g(V) = \beta V$ if $V > 0$ where $\alpha = \frac{R_0}{R_6}$ and $\beta = \frac{L_1 + L_2}{L_2}\frac{R_0}{R_6}$ control the shape and location of the W-nullcline [11].

Note also that the initial condition U_{ini} can be loaded in the neuron via an analogue commutator controlled by V_{syn}.

Although it is usual to study a system with normalized variables, it is more convenient to describe electrical circuits with experimental variables. Therefore, we will keep both variables (as normalized V and experimental U) in the following of this paper.

In the case $\alpha = \beta = 1$, the system corresponds to the standard FitzHugh-Nagumo equation (with diffusive parameter set to zero) where nullclines can only intersect at a single equilibrium point leading to Andronov-Hopf bifurcations.

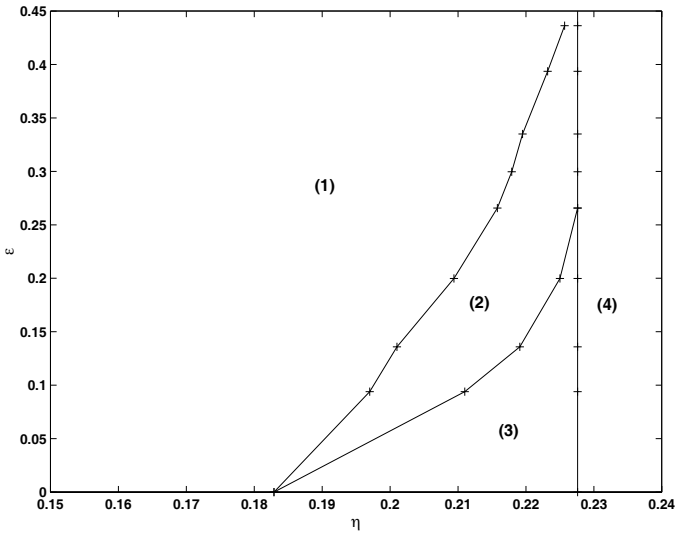

Figure 3. Bifurcation curves in the dimensionless plane (η, ε)

In the general case $\alpha \neq \beta$, three equilibrium points $O_1(V^{(1)}, W^{(1)}), O_2(V^{(2)}, W^{(2)})$ and $O_3\left(V^{(3)}, W^{(3)}\right)$ are expected, as illustrated in Figure 2, from which an experimental

phase portrait (V,W) can be deduced by rescaling the x-axis by a factor $1/\gamma$ and the y-axis by a factor $1/R_0$.

In this case, the parameters are $\alpha = 0.5$, $\beta = 1.96$ and $\eta = 0.226$. We can note that this phase portrait is very similar to the one occurring from the modified Morris-Lecar equations [5] proposed to model barnacle muscle fibers and pyramidal cells.

As expected by the stability analysis of equation (2), several results are to be distinguished depending on the location of the three fixed points and on initial conditions [11].

Keeping parameters of Figure 2, i.e. $\alpha = 0.5$ and $\beta = 1.96$, an experimental determination of the bifurcation curves in the parameter plane (η, ε) is proposed in Figure 3.

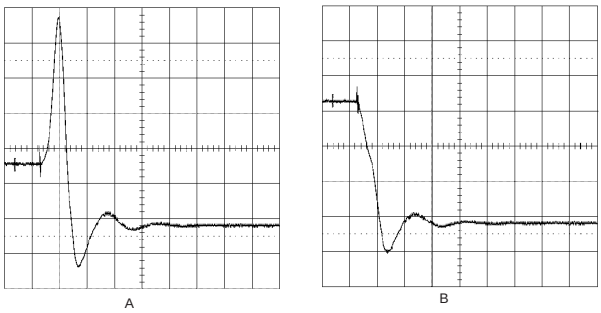

Figure 4. Excitation threshold corresponding to domain (1) of Figure 3 with $\eta = 0.19$ and $\varepsilon = 0.2$ ($E_1 = 0.332\,V$ and $C = 1\,nF$).
Excitation pulse (oscillogram on the left) and perturbation reaching the resting state (oscillogram on the right).
Abscissa 20 μs per division; ordinate 225 mV per division.

In the domain (1), the points O_1 and O_3 are stable and unstable foci, while O_2 is a saddle.

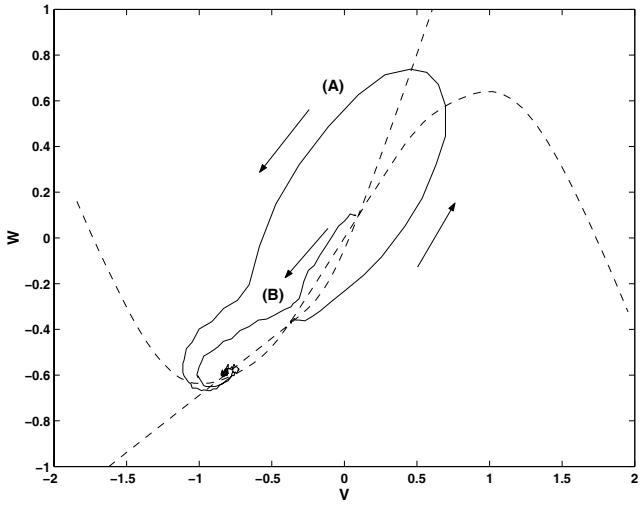

Figure 5. Dimensionless phase plane (V,W) showing stability with excitation threshold corresponding to domain (1) of Figure 3 with $\eta = 0.19$ and $\varepsilon = 0.2$ ($E_1 = 0.332\,V$ and $C = 1\,nF$).

Therefore, if a perturbation of the rest state O_1, is large enough so that it lies between the points O_2 and O_3, the system responds with an excitation pulse, otherwise it decays to the resting state O_1, as illustrated in Figure 4.

The left oscillogram (A) shows an excitation pulse while the right one (B) shows a perturbation reaching the resting state, as its initial condition is above O_3.

Figure 5 gives the experimental phase portrait for the both cases with A (resp. B) corresponding to the oscillogram on the left (resp. right) in Figure 4.

Domain (2) corresponds to the bistability case characterized by the existence of a stable fixed point O_1 and a stable limit cycle that has appeared from a big homoclinic loop bifurcation. Then, the model exhibits oscillations if the perturbation is large enough, as illustrated in Figure 6.

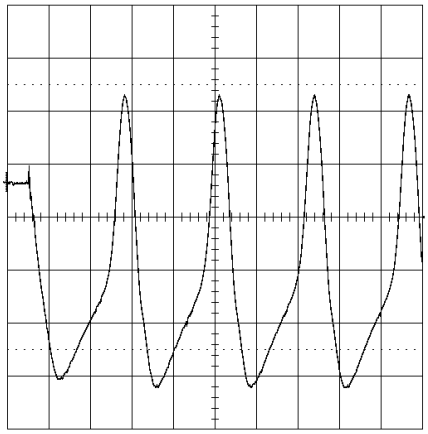

Figure 6. Experimental spiking train of pulses, with $\eta = 0.22$ and $\varepsilon = 0.2$ ($E_1 = 0.3876\,V$ and $C = 1\,nF$).
Abscissa 20 μs per division; ordinate 195 mV per division.

The Figure shows a spiking train of pulses corresponding to the limit cycle in the experimental phase portrait presented in Figure 7. Otherwise, it decays to the rest state, as in domain (1) but only if its initial condition is under O_2.

In domain (3), the fixed point looses stability via a subcritical Andronov-Hopf bifurcation and only oscillations occur in the model, which are similar to the spiking train of pulses of Figure 6. Note that in the region (2), another saddle homoclinic loop bifurcation has taken place leading to a small unstable limit cycle near the fixed point O_1. Due to instabilities, we can not distinguish this bifurcation experimentally. Experiments have shown that, contrary to standard FHN, arbitrarily long interspike intervals can be found, as the two lower equilibrium points are merging.

Finally, in domain (4), a single unstable fixed point O_3 exists leading to oscillations as illustrated in Figure 8.

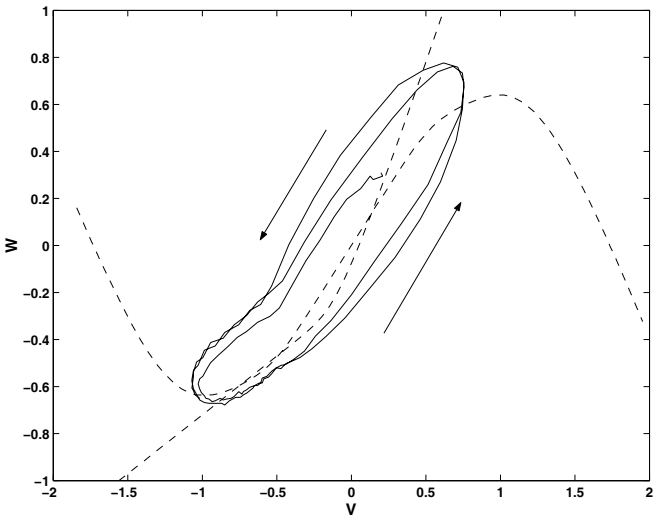

Figure 7. Dimensionless phase plane (V,W) showing bistability corresponding to domain (2) of Figure 3, with $\eta = 0.22$ and $\varepsilon = 0.2$ ($E_1 = 0.3876\,V$ and $C = 1\,nF$).

Note that the existence of these domains has been confirmed with numerical simulations and stability analysis of equation 2.
Increasing ε above 0.5 would imply about ten other domains. Nevertheless, these features are not necessary to develop a wide range of dynamical behaviors, as described in the following section.

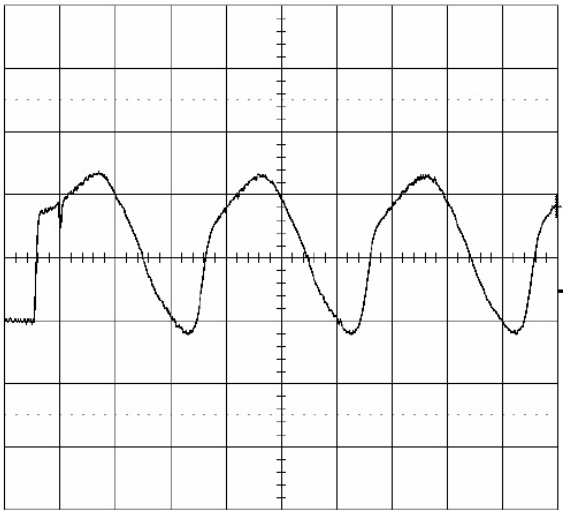

Figure 8. Oscillations corresponding to domain (4) with $\eta = 0.296$ and $\varepsilon = 0.2$
($E_1 = 0.521\,V$ and $C = 1\,nF$).
Abscissa 10 μs per division; ordinate 500 mV per division.

UNIDIRECTIONAL COUPLING OF TWO CELLS

The neurons communicate mainly between them through specialized devices called synapses via chemical messages. The chemical synapse transmits the impulse unidirectionally.

Therefore, it is interesting to conceive and to realize an electrical circuit including the same features as the synaptical coupling. We present in Figure 9 the unidirectional coupling between two cells leading to a master-slave configuration where N_i ($i = 1,2$) are described by the circuit of the Figure 1.

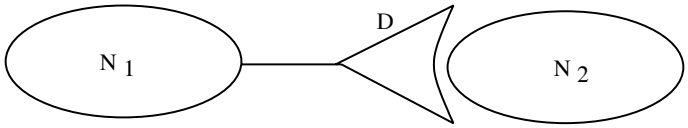

Figure 9. Coupling between two cells N_1 and N_2.

Let us introduce D the coupling parameter (synaptic strength).
Its electrical circuit, as illustrated in the Figure 10, includes an adder-inverter, an inverter and then a follower.

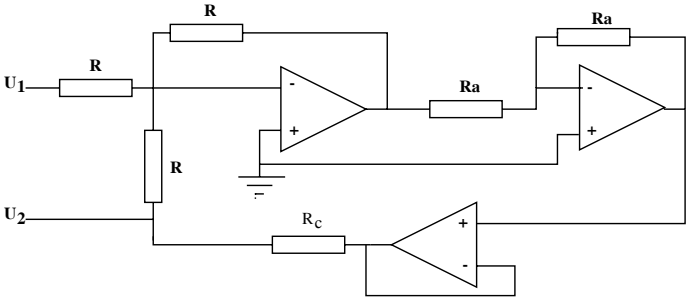

Figure 10. Unidirectional coupling circuit.

U_1 (resp. U_2) is the voltage capacitor of the cell N_1 (resp. cell N_2). The value of the resistor R is fixed to $100\ k\Omega$, which is large compared to the other components so that the current going though $2R$ is negligible, $R_a = 10\ k\Omega$, while R_c is a detuning parameter which allows to control the coupling parameter value. Using Kirchoff's laws, the normalized equations corresponding to the schematic configuration in Figure 10 can be expressed by:

$$\begin{cases} \dfrac{dV_i}{d\tau} = \left[V_i - \dfrac{V_i^3}{3}\right] - W_i + DV_i\delta_{2,i} \\ \dfrac{dW_i}{d\tau} = \varepsilon_i\left[g(V_i) - W_i - \eta_i\right] \end{cases} \qquad (3)$$

with $i = \{1,2\}$, and where $D = \dfrac{R_0}{R_c}$ is the unilateral coupling, $\delta_{2,i}$ is a Kronecker symbol, so that $\delta_{2,1} = 0$ and $\delta_{2,2} = 1$.

Therefore, the two neurons are coupled so that a part of current weighted by D via R_c, and generated by N_1 is included in N_2.

The two neurons are initially set to voltage $U_1 ini$ and $U_2 ini$, due to the analogue commutators controlled by voltage $Vsyn$, as illustrated on the Figure 11.

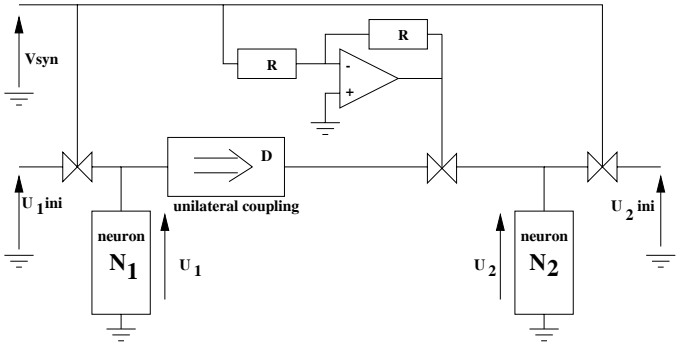

Figure 11. Commutation circuit.

When the initial conditions are loaded, these commutators are switched off while the two neurons are connected via a third commutator controlled by $\overline{Vsyn}$.

Note that the time delay between the two neurons has not been taken into account in this circuit, a master-slave configuration rendering it unnecessary.

The master in a resting state

When the voltage is so that V_1 is constant (the cell N_1 is in a resting state), it is straightforward to show that the variable W_2 and the bifurcation parameter η_2 of the cell N_2 are given by:

$$\begin{cases} \eta_2(D,V_1) = \eta_2(D=0) - DV_1 \\ W_2(D,V_1) = W_2(D=0) + DV_1 \end{cases} \quad (4)$$

where the parameters ε, α, β, η, R_0 and the variables V, W have been defined in the first part.

Therefore, it implies a modification of the excitability of the cell N_2, that is a shift in the (η, ε) plane as illustrated on Figure 12.

The initial conditions are so that, when $D = 0$, the master neuron N_1 lies in domain (1) in the resting state O_1, while the slave neuron N_2 is in domain (3) and generates a spiking train of pulses. When the unilateral coupling is increased and reaches a critical value, the neuron N_2 ceases to oscillate and stays in the resting state O_1, meaning that the slave neuron has been moved from domain (3) to domain (1) of Figure 3.

The ability of neuron N_1 to inhibit neuron N_2 corresponds to the shift predicted by equation (4): As $V_1 < 0$, increasing D implies to increase $\eta_2(D,V_1)$ and therefore the bifurcation curves of Figure 3 are translated along abscissa, while the value of η_2 defined by the electrical parameters of neuron N_2 has not been changed.

This result suggests that, for a defined activity of a slave neuron, the strength of a unilateral coupling should be above a critical value to give to the master neuron the control on the slave neuron.

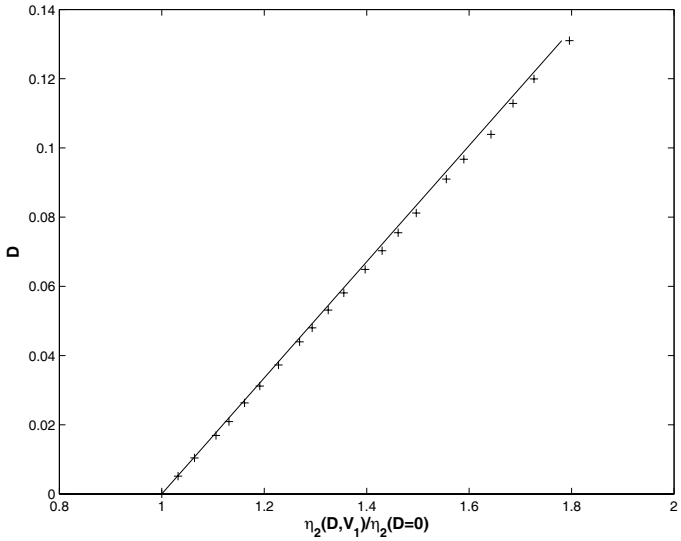

Figure 12. Shifted bifurcation curve of the slave neuron N_2 between domains (1) and (3).
Parameters: Master neuron N_1: $\alpha_1 = 0.5$, $\beta_1 = 1.96$, $\varepsilon_1 = 0$, $\eta_1 = 0.01$ leading to $V_1 = -1.05$ (*i.e.* $U_1 = -921\,mV$)
Slave neuron N_2: $\alpha_2 = 0.5$, $\beta_2 = 1.96$, $\varepsilon_2 = 0$

In Figure 12, experimental values $(D, \eta[D,V_1])$ correspond to the shifted bifurcation curve between domains (1) and (3) of the neuron N_2 with $\varepsilon_2 = 0$ and when the master neuron N_1 lies in domain (1) in a resting state so that $V_1 = -1.05$.

Comparison shows a good match between experimental results and equation (4), validating the unilateral coupling circuit.

The master in a spiking regime

In this section, we present some results when the master is in domain (2) and oscillates. As V_1 is varying in time, we cannot express a simple relationship between the parameters of neuron N_2 and V_1, as in equation (4). Nevertheless, oscillations of neurons N_1 let V_1 be alternatively positive and negative, which implies that the bifurcation curves of neurons are translated along the abscissa in the plane (η, ε) in a periodic manner (the position of saddle points of the cell N_2 is moved periodically).

Thus, the slave neuron N_2 initially situated in the vicinity of a bifurcation curve may be able to cross sometimes this curve and develop a different dynamical behaviour.
Therefore we have investigated the unilateral coupling influence on N_2, in the case when neuron N_1 is initially (*i.e.* when $D = 0$) in domain (3) and oscillating, while the slave neuron N_2 is in domain (1) in its resting state O_1.

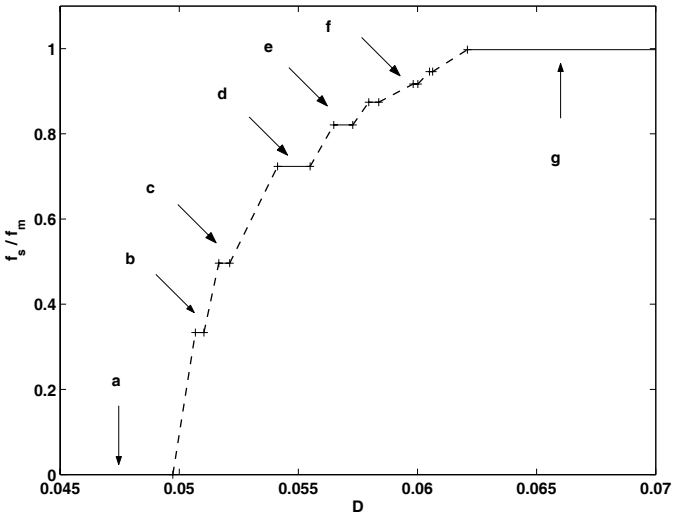

Figure 13. Normalized eigen interspike slave frequency f_s by interspike master frequency f_m versus D with $C = 0\ nF$, $\varepsilon_1 = \varepsilon_2 = 0$, $\eta_1 = 0.199$ and $\eta_2 = 0.109$.

According to the value of D, several different dynamical behaviours can be identified, as illustrated in Figure 13 and 14:
- In case **a**, the coupling strength is small, leading to subthreshold oscillations of f_m frequency, which are not taken into account in Figure 13 but observable in Figure 14.
- In cases **b** to **f**, stable periodic oscillations appear whose eigen interspike frequency follows a devil's staircase-like curve. Only specific values of f_s / f_m are obtainable.
Increasing the coupling strength causes the period-doubling in the slave cell, that is the period is multiplied by 2, 4, 8, 16 and so on.
- In case **g**, N_2 is fully synchronized with N_1. The slave neuron oscillates in the same manner than the master one.

The slave neuron shows also a chaotic sequence of spikes resulting with variable interspike intervals. This chaotic regime, corresponding to the dot lines in Figure 13, between the period-doubling plateaus, is so that the interspike slave period is varying during the experiments. When the coupling parameter is gradually increased, we firstly proceed from a periodic spiking regime to a chaotic regime via a sequence of period-doubling bifurcations. Finally, it leads to the reappearance of periodic dynamics inserted in the chaotic zones.

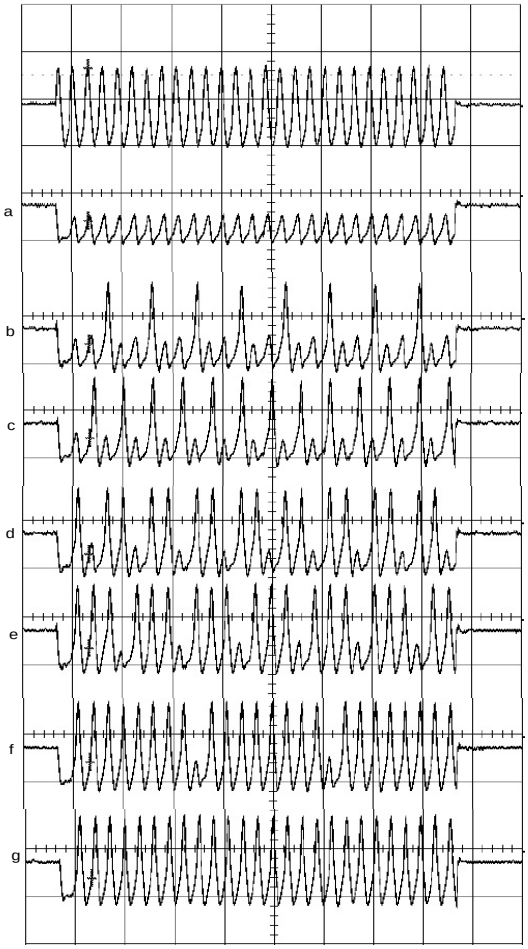

Figure 14. Temporal evolution of experimental voltage U_2 for different values of D corresponding to cases (**a-g)** of Figure 13. Voltage of the master neuron N_1 is shown on top. Abscissa: 0.1 ms per division; ordinate: 1 V per division.

The chaotic puffs disturb the periodic spiking regime. This is intermittency. These disturbances appear in an irregular manner.

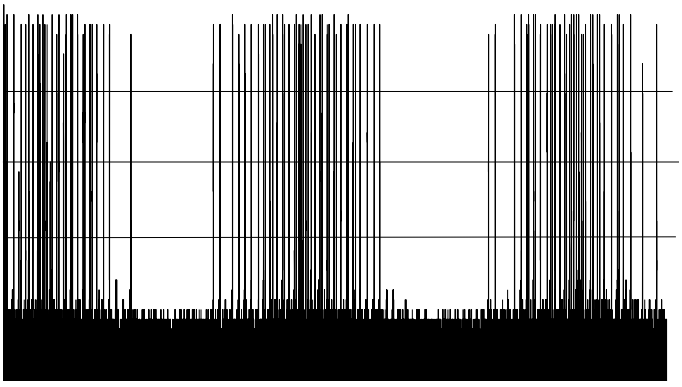

Figure 15. Chaotic signal in the case where $D = 0.0535$ Abscissa: 5 μs per division; ordinate: 1 V per division.

Increasing the coupling parameter causes the increase of the frequency disturbances and then the chaos dominates the regime in the slave cell [8,9].

An illustration of a chaotic signal is given in Figure 15 for $D = 0.0535$. The corresponding probability of normalized interspike slave frequency f_s / f_m is presented on Figure 16. This figure shows that in a chaotic regime, the interspike frequencies f_s are distributed widely in the range $[0, 0.4 f_m]$.

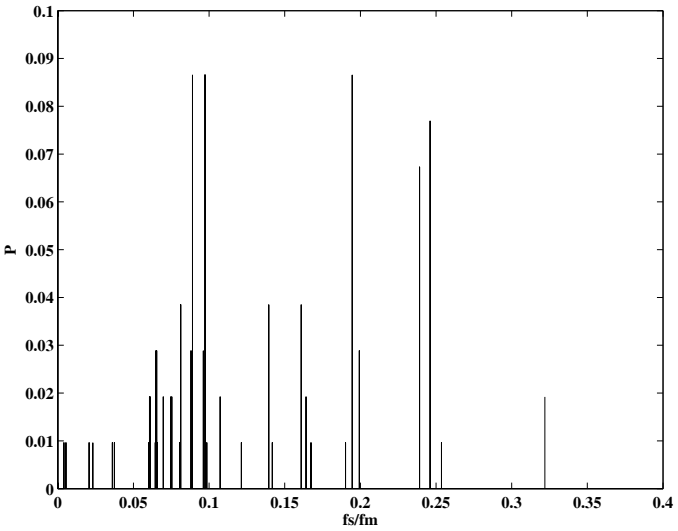

Figure 16. Normalized distribution of the interspike frequency of N_2 corresponding to the signal in Figure 15.

These experiments show that the unilateral coupling strength controls the slave neuron, from a silent to a chaotic dynamical behaviour.

CONCLUSION

A nonlinear electrical circuit has been reported showing the generation of either Andronov-Hopf bifurcations or saddle homoclinic loop bifurcations, which may render it useful in neural modelling as a basic cell for neural network. Furthermore, an integration of such a circuit using inductor-like components could be realized, giving this opportunity of very large scale network.

Futhermore, we have considered the case of two coupled cells, in a master-slave configuration. We have shown that the intervals between successive spikes can be chaotic and depends on the coupling strength. We suggest that this study can be helpful in understanding the different dynamics of potential propagation in brain cells. To complete this work, it would be of interest to study the bidirectional coupling, corresponding to the electric synapse case, and the influence of the size of the network on the fractal dimension of the information [10].

ACKNOWLEDGMENTS

This research has been supported by the Russian-French program of joint research (grant 04610PA), the Russian Foundation for Basic Research (grant 03-02-17135) and INTAS grant (YSF 2001-2/24).

REFERENCES

[1] A.C. Scott. *Neuroscience: A mathematical prime*r, Springer-Verlag, New York, 2002.

[2] C. Koch. *Biophysics of computation: Information processing in single neurons*, Oxford University Press, Oxford, 1998.

[3] J. Nagumo, S. Arimoto and S. Yoshizawa, An active impulse transmission line simulating nerve axon, *Proc. IRE* 50 (1962) 2061-2070.

[4] E.M. Izhikevich, Neural excitability, spiking and bifurcations, *Int. J. Bifurcation and Chaos* **10** 6 (2000) 1171-1266.

[5] J. Rinzel and B. B. Ermentrout, Analysis of neural excitability and oscillations, In *Methods in neuronal modeling, C. Koch and I. Segev editors*, second edition, MIT press, Cambridge, Massachusetts (1998) 251-292.

[6] V. B. Kazantsev, Selective communication and information processing by excitable systems, *Phys. Rev. E* **64** (2001) 056210.

[7] S. P. Dawson, M. V. D'Angelo and J. E. Pearson, Towards a global classification of excitable reaction-diffusion systems, *Phys. Lett. A* **265** (2000) 346-352.

[8] E. Ott, C. Grebogi and J. A. Yorke, *Phys.Rev.Lett.* **64** (1990) 1196-1199.

[9] A. H. Nayfeh, B. Balachandra, Applied nonlinear dynamics, *Wiley-Interscience Publication*, New York, 1995.

[10] V. B. Kasantsev, V. I. Nekorkin, S. Binczak, J. M. Bilbault, Spiking patterns emerging from wave instabilities in a one-dimensional neural lattice, *Phys. Rev. E* **68** (2003) 017201,1-4.

[11] S. Binczak, V. B. Kasantsev, V. I. Nekorkin, J. M. Bilbault, Experimental study of bifurcations in modified FitzHugh-Nagumo cell, *Electronics Letters* **39** (2003) 961-962.